

## Long-range and superfast trapping of DNA molecules in an ac electrokinetic funnel

Jiong-Rong Du, Yi-Je Juang, Jie-Tang Wu, and Hsien-Hung Wei<sup>a)</sup>

*Department of Chemical Engineering and Center for Micro/Nano Science and Technology, National Cheng Kung University, Tainan 701, Taiwan*

(Received 9 September 2008; accepted 3 November 2008; published online 5 December 2008)

In this work we report a microfluidic platform capable of trapping and concentrating a trace amount of DNA molecules efficiently. Our strategy invokes nonlinear electro-osmotic flow induced by charge polarization under high-frequency ac fields. With the asymmetric quadrupole electrode design, a unique converging flow structure can be created for generating focusing effects on DNA molecules. This focusing in turn transforms into a robust funnel that can collect DNA molecules distantly from the bulk and pack them into a compact cone with the aid of short-range dipole-induced self-attraction and dielectrophoresis. Our results reveal that not only can DNA molecules be concentrated within just a few seconds, but also they can be focused into threads of 1 mm in length, demonstrating the superfast and long-range trapping capability of this funnel. In addition, pico M DNA solutions can be concentrated with several decades of enhancement without any continuous feeding. Alternating concentration and release of DNA molecules is also illustrated, which has potentials in concentrating and transporting biomolecules in a continuous fashion using microdevices. © 2008 American Institute of Physics.

[DOI: [10.1063/1.3037326](https://doi.org/10.1063/1.3037326)]

### I. INTRODUCTION

In the recent research and development of nanotechnology microtechnology, considerable efforts have been aimed at separation, sensing, and detection in various chemical and biological applications under Micro Total Analysis Systems ( $\mu$ TAS).<sup>1</sup> Since usual microchip-based analyses contain just trace amounts of samples, a reliable detection must hinge not only on whether samples can be significantly preconcentrated for rendering higher detection accessibility, but also on if the process is efficient at work. Along this line, a number of strategies have been developed for concentrating dilute analytes, for example, through utilizing electrokinetic and chromatographic techniques,<sup>2,3</sup> and embedding miniaturized preconcentrators (e.g., addressable electrodes, monolithic polymer gel, and nanoporous membranes, etc.).<sup>4-8</sup> Yet, it usually takes a relatively long time, up to minutes or even hours, for most of these techniques to attain apparent concentration enhancement, which could set a “bottleneck” to subsequent detections and hence be less desirable for certain applications.

Compared to these methods, high-frequency ac electrokinetics<sup>9</sup> has recently emerged as a very effective means to drive fluids and transport samples in microscales because it not only can prevent bubbles due to Faradaic reactions but also possesses a diversity of manipulation capacities. Since the phenomena typically occur at frequencies ranging from kilohertz to megahertz, rapid charging and discharging by ac fields cause polarization far from the Poisson-Boltzmann equilibrium. When this polarization occurs at the proximity of energized electrodes, nonlinear ac electro-osmotic flow (ACEO) can be set up with velocity scale.<sup>10</sup>

---

<sup>a)</sup> Author to whom correspondence should be addressed. Electronic mail: hhwei@mail.ncku.edu.tw.

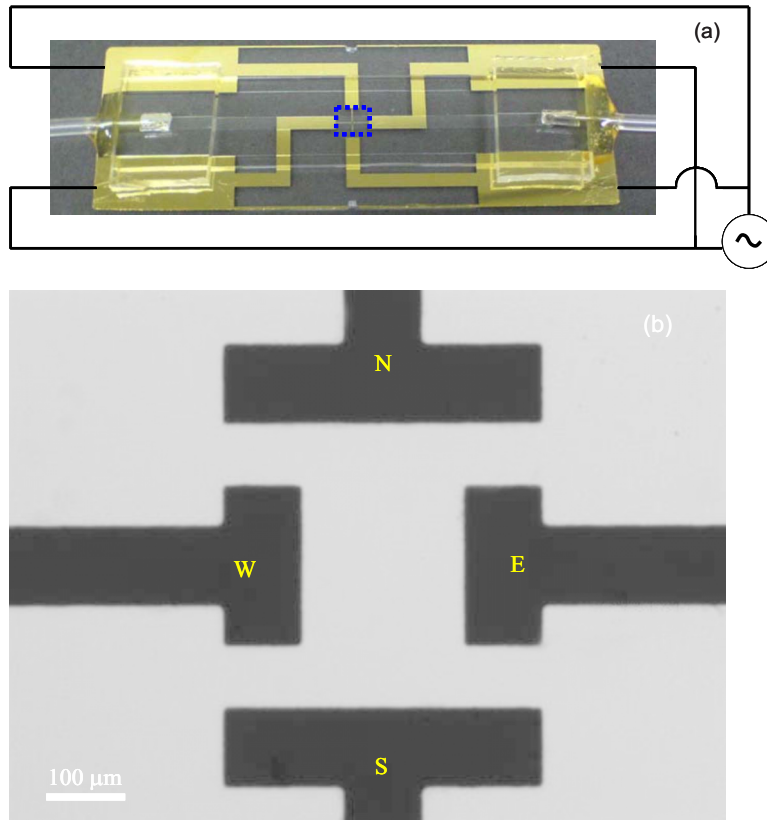


FIG. 1. (a) Featured microdevice. (b) Enlarged view of quadrupole electrode system highlighted in (a).

$$U \sim \chi \frac{\varepsilon V^2}{\eta L}, \quad (1)$$

where  $\varepsilon$  and  $\eta$  stand, respectively, for the permittivity and viscosity of the working fluid, and  $V$  the applied voltage across the electrode separation  $L$ . Here  $\chi$  is the dimensionless prefactor of  $10^{-3}$ – $10^{-2}$  by accounting for the effects of the electrode dimension and applied frequency, so that a more accurate estimate for the ACEO velocity can be obtained in magnitude consistent with the measured values.<sup>10</sup>

As ACEO usually appears in the vortex form, it can be used in trapping DNA molecules<sup>11</sup> or in concentrating pathogens for enhancing detection susceptibility.<sup>12</sup> In addition, it offers an advantage of engineering flow with suitable electrode designs. In our recent work, we employed an asymmetric quadrupole electrode design and found a unique ACEO structure that has potentials in manipulation of colloids or biomolecules.<sup>13</sup> In this article, we would like to employ the same electrode design for trapping DNA molecules with ac fields. As we shall show below, this design is capable of concentrating a trace amount of DNA molecules such as pico M very efficiently.

## II. EXPERIMENTAL SECTION

The featured quadrupole electrode system consists of four T-shaped electrodes, as shown in Fig. 1. These electrodes frame a rectangular region in the central area of the device, and are arranged in such a way that the north and south electrodes act as the working electrodes and the east and west ones as the counterelectrodes, or vice versa. The gold electrodes were patterned on the glass substrate via electron-beam sputtering followed by photolithographic process and wet etching. The inner area surrounded by the four T-shaped electrodes is  $200 \times 350 \mu\text{m}^2$ . The gap between the adjacent electrodes is  $75 \mu\text{m}$ . The PDMS microchannel with 1 mm in width and

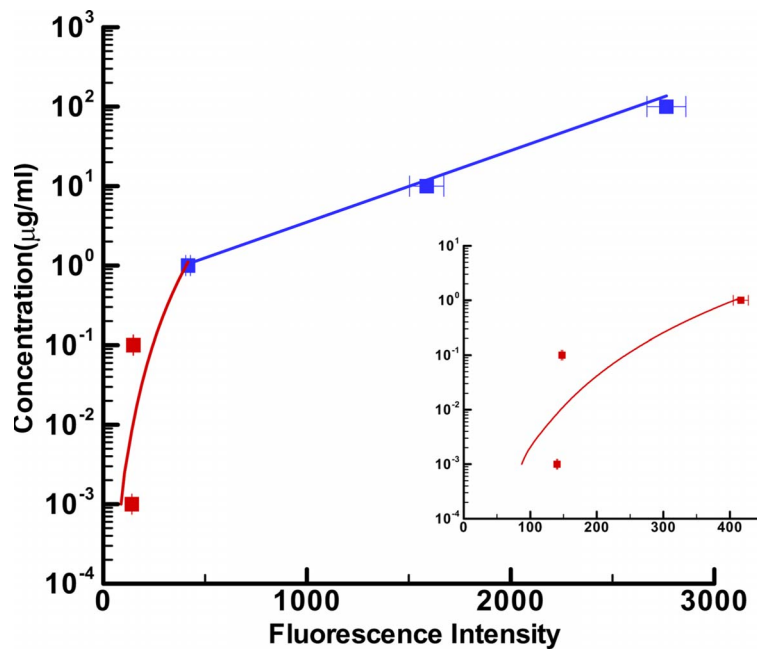


FIG. 2. Dependence of fluorescence intensity on DNA concentration. The lines are the best fitted.

60  $\mu\text{m}$  in depth was sealed to the glass slide after oxygen plasma exposure. The device was connected to a function generator (Agilent 33220A) which provides ac fields with tunable voltage and frequency.

Various T4 DNA (Wako,  $MW=1.076 \times 10^8$ ) solutions of concentrations ranging from  $10^{-3} \mu\text{g/ml}$  ( $10^{-2}$  pM) to  $1 \mu\text{g/ml}$  (10 pM) were prepared in the  $10^{-3}$  M Tris-HCl buffer with addition of 1% beta-mercaptoethanol. The T4 DNA molecules were intercalated with YOYO-1 fluorescence dye with the basepair-to-dye ratio of 5:1. The conductivity of these DNA solutions is approximately  $150 \mu\text{S/cm}$ . The corresponding double-layer thickness  $\lambda$  is about 10 nm. The DNA solutions were first filled into the microchannel by using a syringe pump (Cole Parmer) and electric fields are then applied at voltages ranging from 5 to 20 Vpp (peak-to-peak voltage). The experiments were conducted around frequency  $D/(\lambda L)$ , the inverse RC time of the system.<sup>10</sup> With  $L \sim 100 \mu\text{m}$  and the ionic diffusivity  $D \sim 10^{-5} \text{ cm}^2/\text{s}$ , this frequency is about 1 kHz.

The motion of DNA molecules was observed using an inverted fluorescence microscope (TE2000-S, Nikon) with  $40\times$  objective lens. A high-resolution, cooled intensified charge-coupled device (CCD) camera (CoolSNAP HQ, Roper Scientific) was employed to capture the movement of DNA molecules illuminated by a fluorescent lamp. The fluorescence intensity was measured in real time with an image processing software (Fryer Metamorph). To quantify the increment in the DNA concentration, a calibration curve was made by measuring the fluorescence intensities at various DNA concentrations in the absence of applied fields, as provided in Fig. 2.

### III. RESULTS AND DISCUSSION

#### A. Hydrodynamic focusing by asymmetric ac electro-osmotic flow

Figure 3(a) shows the apparent trapping of DNA molecules around the periphery of the central electrode area. The most concentrated spots occur at the east and west electrodes wherein DNA molecules are focused into compact cones near the intersection of the horizontal and vertical electrodes. For the north and south electrodes, however, there is no clear formation of such spots, as will be explained later. In addition, the phenomenon is accompanied by two concentrated DNA threads of 1 mm in length along the east and west electrodes. This finding suggests that a dilute DNA sample can be concentrated within a volume of  $\sim 1 \text{ mm} \times 1 \text{ mm} \times 100 \mu\text{m} = 100 \text{ nl}$ , which

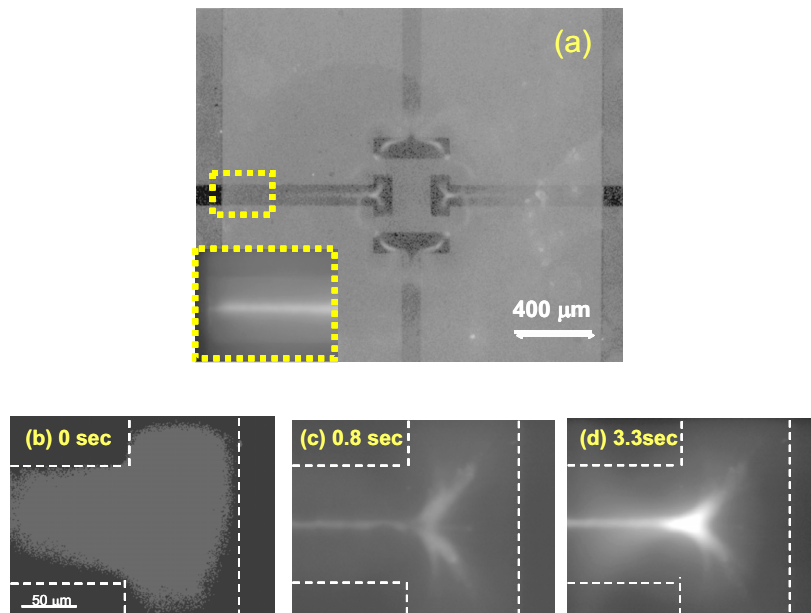


FIG. 3. (a) Long-range electrokinetic funnel under an ac field of 20 Vpp (peak-to-peak voltage) at 1 kHz. The DNA concentration is  $1\mu\text{g/ml}$ . The inset is the blow-up view of a 1 mm-long concentrated DNA thread. The sequential images on the west electrode in (a) are taken at (b) 0.0, (c) 0.8, and (d) 3.3 s after turning on the field.

is about 100 times that of a  $100\text{-}\mu\text{m}$ -sized, dropletlike sample commonly used in  $\mu$  TAS. Moreover, this concentration process can be achieved without needs in continuous sample feeding, as opposed to other methods.<sup>3</sup>

Figures 3(b)–3(d) show the sequential images of the trapping process at the west electrode. Upon applying an ac field, two separate streams emit obliquely from the vertical portion of the electrode and then quickly meet in the middle [Figs. 3(b) and 3(c)]. Since this converging streaming admits a local stagnation-point flow near the merging point, it draws DNA molecules from the bulk toward the point. Also because there must exist a precipitous drop of the velocity near the merging point, it in turn focuses the DNA molecules into a bright and compact conical spot above the electrode surface [Fig. 3(d)]. As there is no continuous supply of DNA molecules to maintain the focusing, the converging flow must be sufficiently fast to oppose inevitable molecular diffusion created by the buildup of DNA molecules in the spot. The effectiveness of this focusing is reflected by the local Peclet number  $\text{Pe} = Ua/D_{\text{DNA}}$ , the ratio of diffusion time  $a^2/D_{\text{DNA}}$  to the flow time scale  $a/U$ , where  $a$  is the size of the focused spot,  $D_{\text{DNA}}$  the molecular diffusivity of T4 DNA, and  $U$  the local velocity scale near the merging point. For the current design with  $a \sim 10\mu\text{m}$ ,  $D_{\text{DNA}} \sim 10^{-9}\text{cm}^2/\text{s}$ , and  $U \sim 10^2\mu\text{m}/\text{s}$ ,  $\text{Pe}$  is about  $10^4$ , suggesting that such hydrodynamic focusing is indeed robust.

It must be emphasized that while DNA molecules can be focused hydrodynamically by the converging ACEO streaming, they cannot be held solely by such a flow, since the flow is divergence-free and DNA molecules could be depleted by the exiting stream after the focusing. In fact, we observe that the focused DNA spots can last as long as tens of seconds and vanish soon after turning off the field, suggesting that some other field-induced effects must be involved, which will be discussed in more detail in Sec. III B.

The observed hydrodynamic focusing can be attributed to asymmetric ACEO vortices generated by our quadrupole electrode system. In general, ACEO, because of the antisymmetric space charge distribution on the electrode surfaces, appears as a pair of microvortices above the electrodes.<sup>10</sup> At frequencies around the inverse  $\tau_c$  time used in our experiments, Ohmic charging dominates and hence sets up the fluid motion from the middle toward the outer edges of the electrodes [Fig. 4(a)]. In our electrode system, since the applied field is acting from the north-

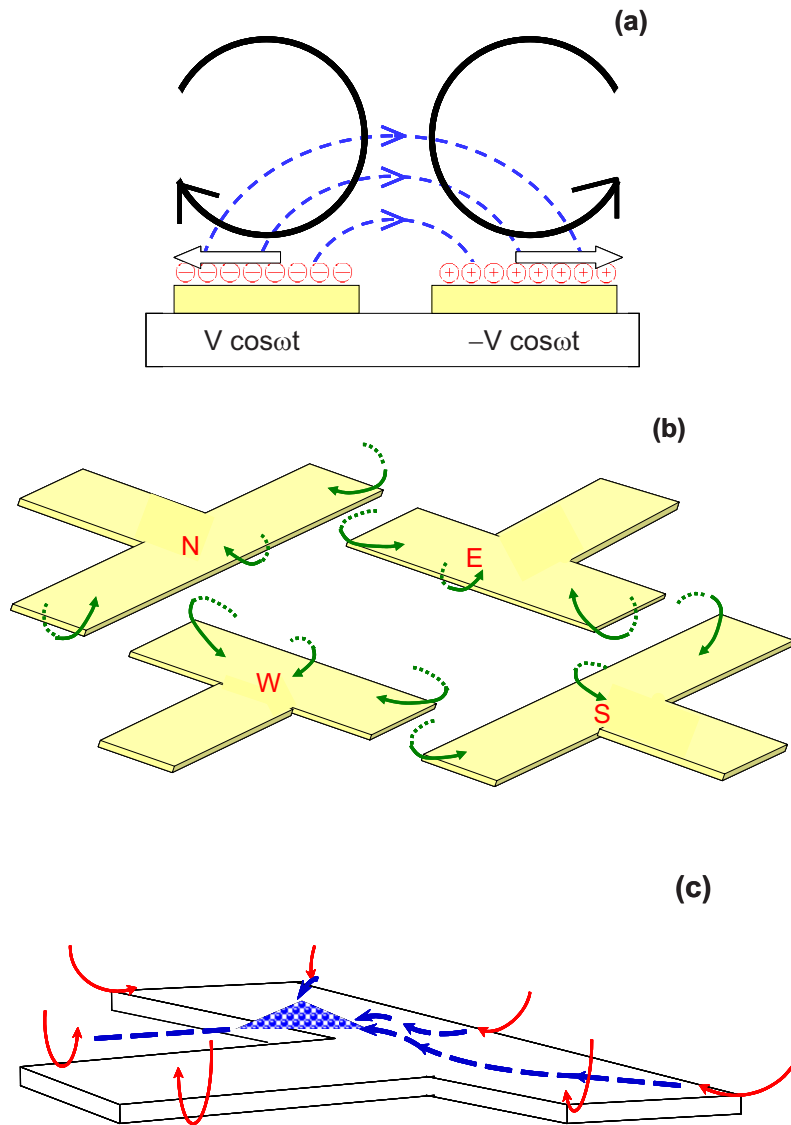


FIG. 4. (a) ac electro-osmotic vortices induced by Ohmic charging on the co-planar electrodes. Black and blue-dashed lines represent the respective directions of the flow and the applied field. White arrows indicate the directions of the counterion movement on the electrodes in response to the applied field. (b) Schematic of the flow (indicated by green) induced by the quadrupole electrode system. Near the electrode edges, the fluid motion is from the bulk (dashed lines) toward the electrode surfaces (solid lines). (c) Mechanism of hydrodynamic focusing occurring on the west electrode. Red and blue lines indicate the fluid and the DNA movement, respectively.

south to the east-west direction or vice versa during a cycle, the induced ACEO vortices will have different sizes and speeds around the inner periphery of the electrodes in response to this quadrupole field [Fig. 4(b)]. As illustrated in Fig. 4(c), the vortices are the strongest near the corners where local electric fields are the highest, but become weaker away from these locations. As these vortices tend to bring DNA molecules from the bulk toward the electrode surface, the effect produces lateral focusing of DNA molecules along the vertical part of the electrode. Since the flow on the horizontal portion can also assist in focusing DNA molecules toward the central line, these two effects combined generate a converging ACEO streaming, which in turn transforms into a unique conduit capable of draining the surrounding DNA molecules into a compact spot.

A similar reasoning might explain why some DNAs can still be focused on the north and south electrodes. These DNA molecules, however, do not appear to form solid concentrated spots as

those on the east/west electrodes. This could be because the north/south electrodes are larger than the east/west electrodes in dimension, making the focusing in the former not as strong as that in the latter.

A few remarks are worth making below. In our previous study,<sup>13</sup> we have demonstrated that the use of the present quadrupole electrode design can produce an asymmetric ACEO structure, which motivates us with its potential use in manipulation of colloids and biomolecules. Here we show that the ACEO generated by the same electrode design can indeed be used to concentrate DNA molecules. The key feature of this flow is that the converging streaming formed at the east and west electrodes can act like a robust “funnel” and hence be capable of focusing DNAs very rapidly.

The concentration effect, however, could be sensitive to the detailed electrode design. If the east and west electrodes were replaced by two large electrode blocks, the effect might not be as efficient as that in the present study, because the funnel—the local converging flow structure—could no longer form in this case.

To increase the area of trapping, it is possible to design two quadrupole electrode sets and arrange them in such a way that the horizontal electrode of one set is connected to that of the other. In this way, the focusing streams created by the two sets will actually be heading on each other, making the concentration effect more effective. The use of such an electrode design for trapping DNA will be explored in our future work.

## B. Dipole-induced trapping of DNA molecules expedited by ACEO focusing

As discussed earlier, it is unlikely to maintain the DNA spots solely by hydrodynamic focusing with the ACEO stream, unless some additional effects are involved. Whatever these effects are must be induced by electric fields, since the spots fade away soon after removing the field. As DNA is a polyelectrolyte and can be polarized by electric fields, there are two plausible field-induced mechanisms responsible for holding the focused spots to against the flow.

One arises from self-attraction between polarized DNA molecules through their dipole-dipole interactions.<sup>15</sup> Since a dipole of strength  $\mu$  possesses energy of  $\mu/4\pi\epsilon r^2$ , it can be shown that the interaction energy between two aligned dipoles of separation  $r$  is  $-\mu^2/2\pi\epsilon r^3$ .<sup>16</sup> With the induced dipole moment  $\mu=2\pi\epsilon R^3 KE$ , this energy reads

$$\phi_{dd} = -8\pi\epsilon R^3 c K^2 E^2, \quad (2)$$

with  $R$  ( $\sim 1 \mu\text{m}$ ) being the size of DNA,  $c=(R/r)^3$  the volume fraction of DNA molecules in the solution,  $K$  the effective polarizability (i.e., the real part of the Clausius-Mossotti factor), and  $E$  the electric field. Here the minus sign signifies attraction resulted from the interactions. Also, the interactions are short-range since  $\phi_{dd}$  decays at the rate of  $r^{-3}$ . In the absence of convection, such dipolar attraction can lead to association of DNA molecules if  $\phi_{dd}$  is comparable to or higher than the thermal energy  $kT$  in magnitude for preventing dispersion due to Brownian motion. With  $c=10^{-4}$ – $10^{-2}$  and  $E\sim 10^3$  V/cm used in the experiment, the ratio  $|\phi_{dd}|/kT$  is an order of unity or larger, indicating that DNAs can indeed be assembled by electric fields through this mechanism. Alternatively, for a given applied field strength, the lower limit of DNA concentration due solely to such self-association between polarized DNA molecules can be estimated by setting  $|\phi_{dd}|\sim kT$  based on the same reasoning above. With the typical field intensity  $E\sim 10^3$  V/cm, we have  $c\sim 10^{-4}$  or about  $10^{-3}$   $\mu\text{g/ml}$ . For detectable concentration enhancement here, DNA solutions range 0.1–1  $\mu\text{g/ml}$ , which is 10–1000 times the lower limit estimated above.

In the presence of flow, however, it is generally difficult to maintain such DNA association since flow could sweep DNA molecules apart. And yet, because of the existence of the converging stagnation point, the ACEO vortices can bring DNAs toward the point near which the flow nearly vanishes, and hence can facilitate the association of focused DNA molecules.

Aside from the dipole attraction, the second effect, dielectrophoresis (DEP)—the motion of a

polarized object under the action of a nonuniform field—can also occur simultaneously, and would become important when DNA aggregates grow into a larger spot, say, of size  $a$ . The DEP force can be described by<sup>9</sup>

$$F_{\text{DEP}} = 2\pi\epsilon a^3 K \nabla |E|^2. \quad (3)$$

If positive DEP (i.e.,  $K > 0$ ) occurs, the effect tends to attract DNA molecules toward the electrode surface near which fields are high. Since the DEP force increases with cubic of the spot size and now acts to oppose the upward fluid motion set by the ACEO funnel, the spot can be held only when the spot becomes large enough and when these two opposite effects are in balance. To see this more clearly, balancing  $F_{\text{DEP}} \sim 2\pi a^3 \epsilon V^2 / d^3$  with the drag force  $F_{\text{ACEO}} \sim 6\pi\eta U a \sim 6\pi\epsilon\chi V^2 a / L$ , we find that the spot size scales as  $a \sim (3d^3\chi/L)^{1/2}$ , where  $d$  ( $\sim 50 \mu\text{m}$ ) is the distance of the spot to the electrode,  $L$  ( $\sim 100 \mu\text{m}$ ) the width of the electrode, and  $\chi = 10^{-3} - 10^{-2}$ . Hence the estimated spot size is about several to tens of micrometers, which agrees with the experimental observation.

Since the two effects mentioned above are typically short-range and manifest mostly when DNAs come close to the electrode surface or near each other, the ACEO focusing here acts to assist in packing DNAs and hence expedites their assembly. Also because both effects work to against depletion by the flow, this explains why the concentrated DNA spot can still be maintained during the focusing. All the three effects combined thus create a unique cooperative trapping process in such a way that DNAs are first brought distantly from the bulk to form compact spots by the ACEO focusing, and then immediately undergo short-range self attraction and DEP due to induced dipoles, resulting in the fast DNA trapping phenomenon observed in the experiment.

### C. Rapid concentration of dilute DNA molecules

To track how the trapping progresses with time as well as to quantify the efficiency of the trapping, Fig. 5(a) shows the temporal evolutions of the fluorescence intensities at different locations of a focused spot during concentrating  $1 \mu\text{g/ml}$  (10 pico M) DNA solution. The intensity at point  $a$  near the merging point (curve  $a$ ) rises rapidly from the background value 400 a.u. to 2200 a.u. within just 2 s, clearly demonstrating an efficient DNA trapping with enhancement of a factor of 40. The intensities at points  $b$ ,  $c$ , and  $d$  also increase but at slower rates. In addition, we observe that the intensity at point  $a$  decreases after reaching a maximum. This is attributed to the propagation of the concentrated spot advected by converging pumping and to subsequent imbalance between injection and ejection of DNA molecules over the moving spot. As a result, the intensities at points  $b$ ,  $c$ , and  $d$  keep increasing while that at point  $a$  continues declining. The phenomenon is also supported by the shift of the maximum intensity during the propagation from point  $a$  to  $d$  (from right to left). For an ultralow DNA solution such as  $0.1 \mu\text{g/ml}$  (pico M), DNA molecules can still be concentrated with enhancement of a factor of 15, as seen in Fig. 5(b).

With the aid of the calibration given in Fig. 2, we use  $C_{\text{max}}/C_0$ , the ratio of the maximum concentration of the spot to the bulk concentration, to quantify the concentration enhancement as a function of applied voltage. The results for both  $0.1 \mu\text{g/ml}$  and  $1 \mu\text{g/ml}$  DNA solutions are also compared. Figure 6 reveals that there exists a threshold voltage at 5 Vpp beyond which an apparent enhancement can be discerned. This is evident because if voltage is too low, it is neither sufficient to form a converging streaming necessary for focusing DNA molecules nor to produce the required dipole-induced attraction and DEP effects. At voltages higher than 5 Vpp, all these effects become strong enough and can readily trap DNA molecules cooperatively, thereby making the concentration increase as the voltage is increased. The enhancement of  $1 \mu\text{g/ml}$  solution is greater than that of  $0.1 \mu\text{g/ml}$  solution. This is because the higher concentration, the more susceptible focused DNA molecules are to being bound through dipole-dipole attraction. In addition, the enhancement for  $0.1 \mu\text{g/ml}$  solution seems saturated at voltages higher than 15 Vpp. This could be attributed to two reasons. First, if the DNA concentration is too low, dipole-induced association between DNA molecules might not be strong enough to keep them from being de-

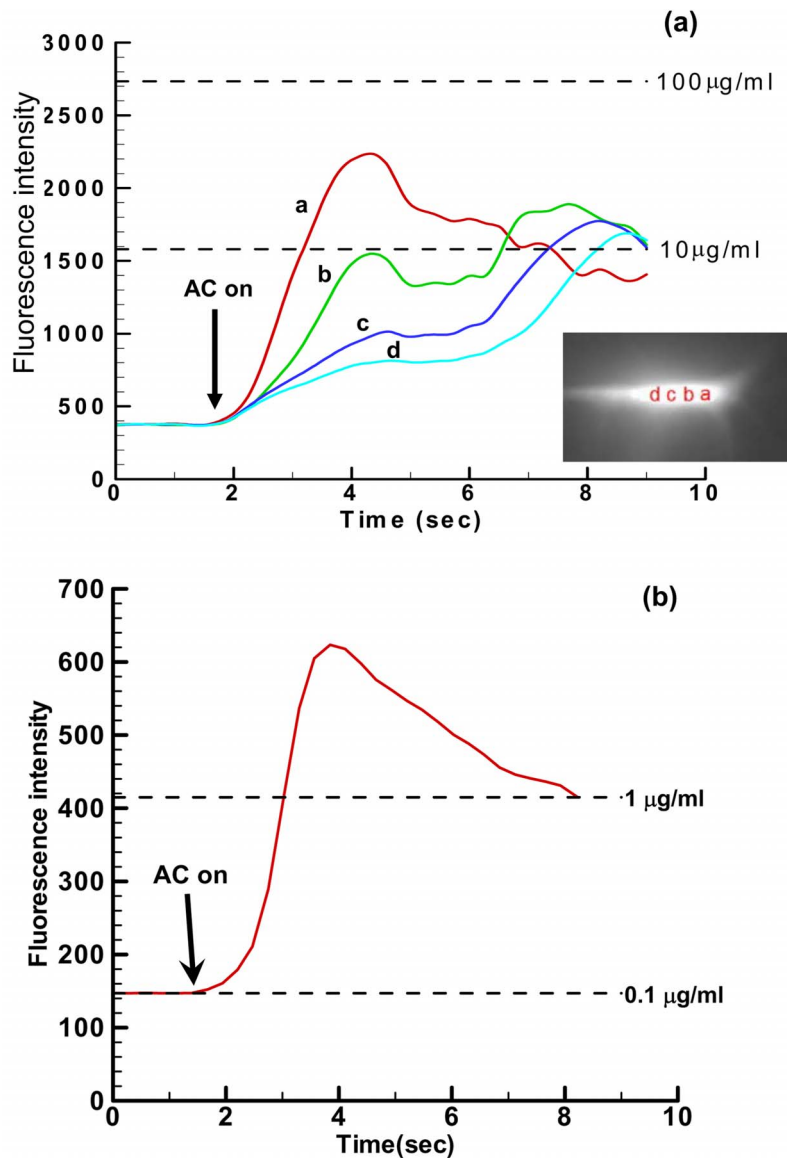


FIG. 5. (a) Evolutions of the fluorescence intensity during concentrating (a)  $1 \mu\text{g/ml}$  (10 pico M) and (b)  $0.1 \mu\text{g/ml}$  (1 pico M) DNA solutions at 20 Vpp and 1 kHz.

pleted by the ACEO stream during the focusing. Second, the amount of DNA molecules left around the trapped spot could be too small to allow further packing of DNA molecules by raising voltage.

It is also worth pointing out that our electrokinetic funnel works at 1 kHz but not at other frequency ranges. At a low-frequency such as 100 Hz, although there is a flow, it is not able to trap DNA molecules. Because at such a frequency Faradaic injection could occur and cause co-ion buildup on the electrodes,<sup>14</sup> the resulting polarization and hence the induced flow direction are opposite to those at 1 kHz. Consequently, rather than being focused toward the electrodes, DNA molecules are swept away by the flow toward the bulk. At a moderately high frequency, say, 10 kHz, a similar trapping phenomenon can be observed, but it is not as effective as that observed at 1 kHz because the flow becomes more sluggish. For frequencies of 100 kHz–1 MHz, there is merely fluid pumping toward the central region, which again does not produce any trapping effects on DNA. Such pumping could be attributed to electrothermal effects arising from permittivity or



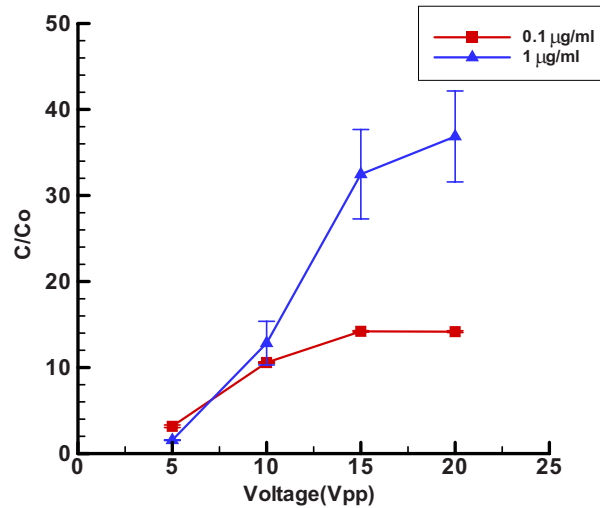


FIG. 6. Effects of applied voltages on the concentration enhancement of dilute DNA solutions.

conductivity gradients near heated electrodes.<sup>17</sup> At much higher frequencies ( $>10$  MHz), there is virtually no fluid motion at all, because the field alternates its polarity too rapidly to cause appreciable polarization over the electrodes for generating ACEO. Although DEP can dominate in this case, it appears less efficient to trap DNA alone since the estimated DEP velocity is about  $10 \mu\text{m/s}$  which is an order of magnitude smaller than the ACEO velocity here.

Aside from the characteristics presented above, our ac funnel possesses another feature: A reversible switch that enables us to trap and release DNA molecules alternately. As is evidenced in Fig. 7, the as-concentrated DNA molecules can be released back to the bulk by turning the field off and then reconcentrated again by turning the field on. When successively turning on/off the field three times, the fluorescence intensity shows the repetitive response of rapid increase (within 5 s) followed by gradual decrease (for 15 s). The slight attenuation of the peak could be attributed to intermixing of the DNA molecules between consecutive concentration/release processes. Such a reversible trap is possible only when the process occurs *above* the electrode surface, which differs

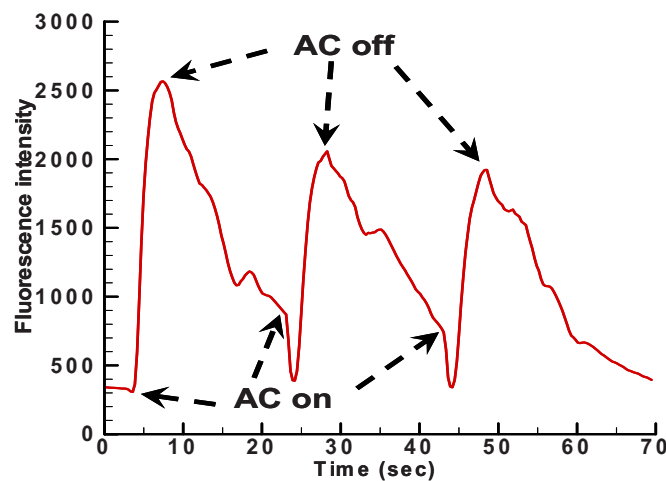


FIG. 7. Evolution of the fluorescence intensity of alternate concentration and release of  $1 \mu\text{g/ml}$  DNA solution with successively turning on and off the field at 20 Vpp and 1 kHz.

from dielectrophoretic trapping<sup>18,19</sup> or colloidal assembly driven by dc fields.<sup>20</sup> This feature not only extends the ability to manipulate suspended DNA molecules, but also prevents them from possible permanent binding (due to surface adsorption or noncovalent forces, for example) to the electrode surface during trapping.

#### IV. CONCLUDING REMARKS

In conclusion, we have demonstrated that the use of the present quadrupole electrode design can create a robust funnel capable of achieving superfast and long-range trapping of DNA molecules with ac fields. The trapping is the result of collaborative effects of ACEO focusing, dipolar attraction between polarized DNA molecules, and DEP. It is shown to have three distinct features. First, significant concentration enhancement can be achieved within seconds. Compared to existing methods, our platform is more efficient in concentrating DNA molecules. Second, because the trapping is typically long range, a trace amount of DNA down to pico M can be concentrated without needs in any continuous sample supply. Finally, the reversible switch between trapping and release of DNA has potentials in concentrating and transporting biomolecules in a continuous fashion.

#### ACKNOWLEDGMENTS

This work was supported by National Science Council of Taiwan under Grant No. NSC 95-2221-E-006-405 of Y.J.J. and Grant No. NSC 97-2628-E-006-001-MY3 of H.H.W. We also thank Professor Shau-Chun Wang of National Cheng Chung University for his helpful discussion.

- <sup>1</sup> P. S. Dittrich, K. Tachikawa, and A. Manz, *Anal. Chem.* **78**, 3887 (2006); H. A. Stone, A. D. Stroock, and A. Ajdari, *Annu. Rev. Fluid Mech.* **36**, 381 (2004).
- <sup>2</sup> C.-H. Lin and T. Kaneta, *Electrophoresis* **25**, 4058 (2004).
- <sup>3</sup> J. Dai, T. Ito, L. Sun, and R. M. Crooks, *J. Am. Chem. Soc.* **125**, 13026 (2003); Y.-C. Wang, A. L. Stevens, and J. Han, *Anal. Chem.* **77**, 4293 (2005).
- <sup>4</sup> J. Khandurina, S. C. Jacobson, L. C. Waters, R. S. Foote, and J. M. Ramsey, *Anal. Chem.* **71**, 1815 (1999).
- <sup>5</sup> C. Yu, M. H. Davey, F. Svec, and J. M. J. Frechet, *Anal. Chem.* **73**, 5088 (2001).
- <sup>6</sup> S. N. Brahmasandra, V. M. Ugaz, D. T. Burke, C. H. Mastrangelo, and M. A. Burns, *Electrophoresis* **22**, 300 (2001); F. A. Shaikh and V. M. Ugaz, *Proc. Natl. Acad. Sci. U.S.A.* **103**(13), 4825 (2006).
- <sup>7</sup> S. M. Kim, M. A. Burns, and E. F. Hasselbrink, *Anal. Chem.* **78**, 4779 (2006).
- <sup>8</sup> A. V. Hatch, A. E. Herr, D. J. Throckmorton, J. S. Brennan, and A. K. Singh, *Anal. Chem.* **78**, 4976 (2006).
- <sup>9</sup> H. Morgan and N. G. Green, *AC Electrokinetics: Colloids and Nanoparticles* (Research Studies Press, Hertfordshire, England, 2003).
- <sup>10</sup> N. G. Green, A. Ramos, A. Gonzalez, H. Morgan, and A. Castellanos, *Phys. Rev. E* **61**, 4011 (2000); A. Gonzalez, A. Ramos, N. G. Green, A. Castellanos, and H. Morgan, *ibid.* **61**, 4019 (2000).
- <sup>11</sup> M. R. Brown and C. D. Meinhart, *Microfluid. Nanofluid.* **2**, 513 (2006).
- <sup>12</sup> Z. Gagnon and H.-C. Chang, *Electrophoresis* **26**, 372 (2005).
- <sup>13</sup> J. T. Wu, J. R. Du, Y. J. Juang, and H.-H. Wei, *Appl. Phys. Lett.* **90**, 134103 (2007).
- <sup>14</sup> D. Lastochkin, R. Zhou, P. Wang, Y. Ben, and H.-C. Chang, *J. Appl. Phys.* **96**, 1730 (2004).
- <sup>15</sup> L. Mitnik, C. Heller, J. Prost, and J. L. Viovy, *Science* **267**, 219 (1995).
- <sup>16</sup> S. Fraden, A. J. Hurd, and R. B. Meyer, *Phys. Rev. Lett.* **63**, 2373 (1989).
- <sup>17</sup> N. G. Green, A. Ramos, A. Gonzalez, A. Castellanos, and H. Morgan, *J. Phys. D: Appl. Phys.* **33**, L13 (2000).
- <sup>18</sup> A. R. Minerick, R. Zhou, P. Takhistov, and H.-C. Chang, *Electrophoresis* **24**, 3703 (2003).
- <sup>19</sup> M. Washizu and O. Kurosawa, *IEEE Trans. Ind. Appl.* **26**, 1165 (1990).
- <sup>20</sup> S. Wang, X. Hu, and L. J. Lee, *J. Am. Chem. Soc.* **129**, 254 (2007).